EurJIC
European Journal of Inorganic Chemistry

Research Article
doi.org/10.1002/ejic.202300344

Chemistry Europe
European Chemical Societies Publishing

www.eurjic.org

Special Collection

Facile Mechanochemical Reduction and Lithium-Ion Doping of Transition-Metal Oxides[**]

Nathan Davison,[a] Tanima Khatun,[a] Isabel Arce-Garcia,[b] Jamie A. Gould,*[b] James A. Dawson,*[a, c] and Erli Lu+*[a]

In memory of Xiaohei Wang, a life-long friend of E. L.

Transition-metal oxides (MO_x) play essential roles in chemistry, catalysis, materials science and metallurgy. The MO_x reduction and doping are two ubiquitous reactions in academic research and industrial manufacturing, but they are notoriously energy-demanding and require harsh conditions (high temperatures, long durations). In this work, facilitated by mechanochemical ball milling, we report a new route to conduct MO_x reduction and doping at room temperature within 20 minutes enabled by mechanochemical ball milling and lithium metal.

Introduction

Transition-metal oxides (MO_x) play crucial roles in small molecule synthesis and catalysis,[1,2] as well as in materials science[3] and metallurgy.[4] MO_x reduction[5] and doping[6] are two essential reactions in all these applications. However, due to the highly stable lattice structures of the MO_x, their reduction and doping are notoriously energy-demanding and present formidable challenges for chemists. In this work, we focus on two widely applied MO_x: nickel(II) oxide (NiO) and cobalt(II,III) oxide (Co_3O_4).

Co_3O_4 reduction and Li^+ doping are essential reactions in Co_3O_4 catalysis[7] and in the preparation of commercial battery materials,[8,9] such as lithium cobalt oxide ($LiCoO_2$, LCO). However, both Li^+ doping and reduction of Co_3O_4 require high temperatures (>600 °C) for several hours.[10,11] Moreover, reduction of Co_3O_4 requires reducing atmosphere (hydrogen/methane/ethanol),[12] hydrogen plasma at >800 °C,[13] or at the nanoscale under strongly electrochemical reduction conditions.[14] Similar harsh conditions (reducing atmospheres, high temperatures, long durations) are also required for the reduction[15,16] and Li^+ doping[17] of NiO. Facile (room temperature and short reaction times) Co_3O_4/NiO reduction and Li^+ doping at preparative scales is highly desirable, as they could potentially pave the way for new low-carbon and sustainable routes toward battery materials and Co-/Ni-based catalysts (such as metallic Co-/Ni-nanoparticles). However, to the best of our knowledge, such facile Co_3O_4/NiO reduction and Li^+ doping reactions are currently unknown.

Mechanochemistry exploits mechanical forces (impact, shearing and pressing) to directly promote chemical transformations.[18] Compared to conventional solution-phase (stirring and heating) and solid-phase (high-temperature calcination) chemical synthetic methods, mechanochemistry features solvent-free and energy efficacy advantages. Mechanochemistry has a long history,[19] with humans unintentionally using grinding to deliver chemistry in the pre-historic ages. This research field had been in hibernation until the 2000s, but the last two decades have witnessed a renaissance and upsurge in mechanochemistry research, driven mainly by the demands for low-carbon, sustainable and energy-efficient chemical synthesis methods.[20] Since then, mechanochemical methods have been used for organic,[21] inorganic/organometallic,[22] polymer[23] and supramolecular[24] chemistry, particularly because of their merits regarding sustainability. With regards to materials science, mechanochemical methods have also been employed to

[a] N. Davison, T. Khatun, Dr. J. A. Dawson, Dr. E. Lu+
Chemistry – School of Natural and Environmental Sciences
Newcastle University
Newcastle upon Tyne, NE1 7RU (UK)
E-mail: erli.lu@newcastle.ac.uk
james.dawson@newcastle.ac.uk
Homepage: www.erlilulab.org
https://sites.google.com/view/jamesdawson/home

[b] Dr. I. Arce-Garcia, Dr. J. A. Gould
Faculty of Sciences
Agriculture and Engineering
Newcastle University
Newcastle upon Tyne, NE1 7RU (UK)
and
X-Ray Diffraction Facility, School of Chemistry, University College London (UK)
E-mail: jamie.gould@newcastle.ac.uk

[c] Dr. J. A. Dawson
Centre for Energy
Newcastle University
Newcastle upon Tyne, NE1 7RU (UK)

[+] Lead author

[**] A previous version of this manuscript has been deposited on a preprint server (https://doi.org/10.26434/chemrxiv-2022-ncw9w).

Supporting information for this article is available on the WWW under https://doi.org/10.1002/ejic.202300344

Special Collection Part of the "EurJIC Talents" Special Collection.

Research Article
doi.org/10.1002/ejic.202300344

synthesize metal oxide nanoparticles[25] and battery materials.[26] However, there is currently no precedent for using mechanochemical methods to promote doping and reduction of transition-metal oxides.

We realize that two challenges must be tackled to eliminate the harsh conditions from the Co_3O_4/NiO reduction and Li^+ doping: (1) a more powerful reductant must be developed; (2) a more efficient energy input must be employed. Based on our experience in Group-1 metal chemistry,[27–29] we hypothesize that lithium metal, which features a strong reducing power (standard redox potential −3.07 V *vs.* standard hydrogen electrode), could act as both a strong reductant and a Li^+ source for doping. Regarding energy input, as abovementioned, mechanochemical ball milling provides a prime choice. It is worth mentioning that directly employing zero-valent metals (s-, p- and d-blocks) in mechanochemical reactions as reductants/catalysts to facilitate challenging organic/inorganic reactions has emerged as a new trend in mechanochemistry research since the 2010s.[30–33] With these hypotheses, we set off to investigate the mechanochemical ball mill reactions between Li metal and Co_3O_4/NiO. The findings are reported herein.

We would like to clarify that, the mechanochemical reactions in this Article should not be confused with classic heat-induced thermite reactions:[34] (1) We use mechanical forces instead of heat as energy input to initiate the reactions. (2) Our reactions are controllable, while the thermite reactions are largely not. (3) We employ Li metal which has not been studied in the thermite reactions.

Results and Discussion

Under argon atmosphere, ball milling reactions between Li metal (ingots or ribbon) and NiO or Co_3O_4 were examined at three different stoichiometric ratios (Li:MO_x = 1:1, 2:1 or 3:1) (see Supporting Information for details). The ball milling frequency and time are key factors that influence the reaction outcomes. We employ a mild 20 Hz frequency to avoid potential thermal runaway. The reactions were conducted in an intermittent manner by stopping the ball milling every 1 to 2 min to check the external temperature of the milling jar. In all reactions, we observed a three to five minutes induction period (jar temperature did not rise), followed by a one to two minutes exothermic reaction period (jar temperature increased to approximately 35–45 °C). The ball milling processes continued after the exothermic period until the total reaction times reached 15 to 20 minutes to ensure that the reactions were completed.

A 1:1 reaction between Li metal and NiO (20 Hz, 20 min) leads to the full consumption of the Li metal, producing a black powder. Powder X-ray diffraction (PXRD) analysis of the resultant black powder on a silicon zero-background sample holder suggests that the main phases are: (1) Ni; (2) Li_2O; (3) unreacted NiO, in an approximate 1:1:1 ratio (Figure 1a & b). Here, NiO is reduced to zero-valent metallic Ni powder, which can be easily separated from the mixture using a magnet. The PXRD sample was sealed on a silicon sample holder using Scotch Magic™ tape. Given the mild conditions, the reaction herein is significantly improved compared with the current high temperatures hydrogen atmosphere NiO reduction conditions.[14,15] Since unreacted NiO presents in the 1:1 reaction, we anticipate that by increasing the Li:NiO ratio, the reaction could be pushed to completion. Indeed, by increasing the stoichiometric ratio of Li metal to 2 and 3 equivalents, the NiO was significantly (2:1 Li:NiO) or totally consumed (3:1 Li:NiO). In summary, enabled by mechanochemical ball milling, we observed facile and clean reductions of Ni(II)O into Ni(0) and Li_2O. On the other hand, Li^+ doping products (e.g., LiNiO[35]) were not observed.

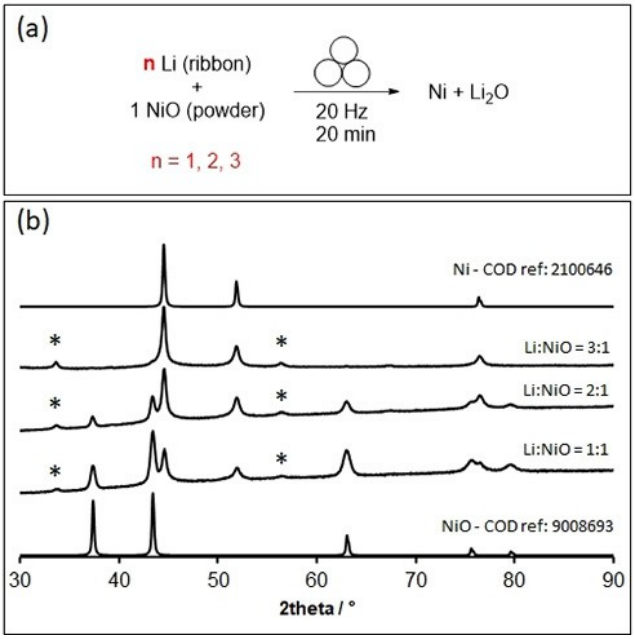

Figure 1. (a) Reactions between Li metal and NiO. (b) Powder X-ray diffraction data of the powdery products from the Li:NiO n:1 (n = 1, 2, 3) reactions. *: Li_2O (COD ref.: 4311895).

Encouraged by the facile mechanochemical reduction of NiO, we expand the methodology into Co_3O_4. Following the same protocols for NiO, mechanochemical reactions between Li metal and Co_3O_4 were conducted at three different stoichiometric ratios (Li:Co_3O_4 = 1:1, 2:1 or 3:1) (Figure 2). The reaction outcomes are more complicated compared to the NiO reactions. We identified Co metal, $Li_xCo_{(1-x)}O$ and CoO as major products, along with other minor products such as LiH and Li_2O (Figure 2a). The approximate product distributions are elucidated in Figure 2a. Co metal, as the reduction product, was also produced at all the three Li:Co_3O_4 ratios. Comparing with the fine Ni metal powder in the NiO reactions, the Co metal was produced as ingots with sizes up to >5 mm (see Supporting Information for details). More interestingly, we observed the formation of mixtures of $Li_xCo_{(1-x)}O$ materials ($0 < x < 0.2$), which is the result of Li^+ doping into Co(II)O. The $Li_xCo_{(1-x)}O$ materials feature a rock salt structure and have been widely investigated as precursors to the mainstream commercial Li-ion battery cathode material LCO.[36]

Research Article
doi.org/10.1002/ejic.202300344

Chemistry Europe
European Chemical Societies Publishing

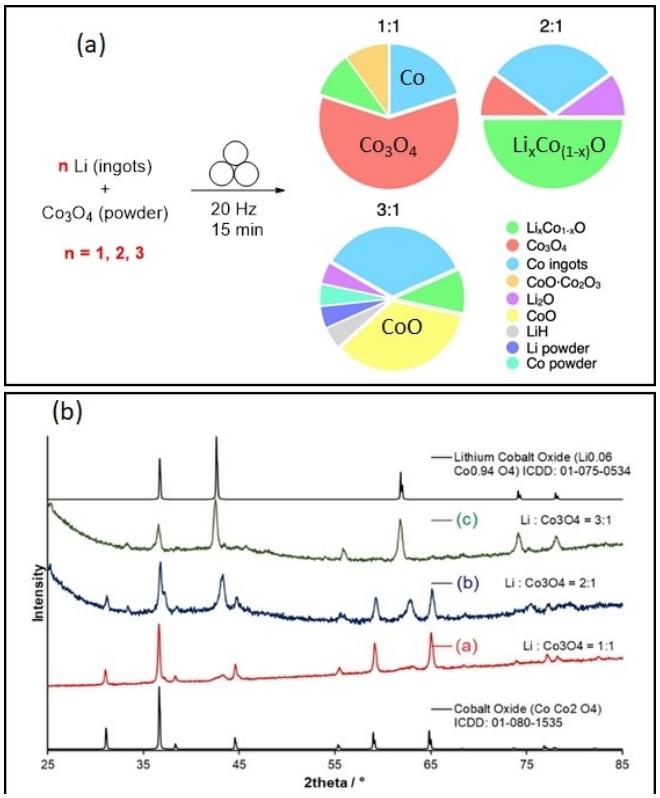

Figure 2. (a) Reactions between Li metal and Co_3O_4 and their approximate product concentrations (wt.%). (b) Powder X-ray diffraction data of the powdery products from the Li:Co3O4 1:1 (a, red), 2:1 (b, blue) and 3:1 (c, green) reactions. Note: The approximate product concentrations (wt%) in Figure 2a were deduced by weighing the magnet-separated Co metal pieces (for Co metal) followed by quantitative phase distribution Rietveld analysis (remaining powder materials).

Specifically, for the 1:1 reaction, the PXRD result suggests that the main phase was unreacted Co_3O_4, with a small amount of $Li_{0.19}Co_{0.81}O$,[37–39] and a second form of Co_3O_4 ($CoO{\cdot}Co_2O_3$). Increasing the Li:Co_3O_4 ratio to 2:1 results in further consumption of Co_3O_4, which was largely converted into Co metal and $Li_xCo_{(1-x)}O$ ($Li_{0.185}Co_{0.815}O$ in this case), along with a minor component of Li_2O. In other word, the increased Li metal stoichiometric ratio facilitated both reduction and doping of Co_3O_4. Further increasing the Li metal ratio to 3:1 led to a dramatic change in reaction pattern. The products from the 3:1 reaction is a mixture of Co metal ingots (15–20 wt.%) and a dark blue powder (80–85 wt.%). The dark blue powder was air sensitive, in contrast to the air-stable black powdery products from the 1:1 and 2:1 reactions. The PXRD data (collected under argon atmosphere) of the dark blue powdery products indicates that it was a mixture of Co(II)O (main), $Li_{0.185}Co_{0.815}O$ (minor), Co (minor), Li (minor), LiH (minor) and Li_2O (minor) (Figure 2b). There is no unreacted Co_3O_4, but instead, with the presence of unreacted Li. In other word, the major reaction pattern in the 3:1 reaction is reduction (producing Co metal and CoO), while the doping pathway (producing $Li_xCo_{(1-x)}O$) is largely suppressed. This finding is crucial, as it indicates that by tuning the stoichiometric ratio of Li metal, it is possible to switch between the reduction and doping reaction pathways. This observation could unlock new avenues to high Li-content $Li_xCo_{(1-x)}O$ materials, which are of significant industrial importance but are currently synthesized *via* energy-intensive protocols.

We conducted density functional theory (DFT) calculations to plot the thermodynamic profiles of the Co_3O_4 reduction and doping reactions, focusing on the formation of $Li_xCo_{(1-x)}O$ materials (x = 0–0.44). Three possible fully balanced reactions are postulated (see Eqs. (S1–S9) in Supporting Information) for each of the three Li:Co_3O_4 ratios considered (Figure 3). As expected, all the calculated reaction energies are strongly exothermic. It is noteworthy that the reactions energies for the three Li:Co_3O_4 ratios are reasonably similar, with values ranging from −1.30 to −1.63 eV per Li. These results suggest that there is little benefit in using high Li metal concentrations (e.g., 3Li:Co_3O_4) in these reactions as the energetic benefit per Li is negligible or is instead an energetic penalty. With regards to the Li^+ doping concentration (x values in $Li_xCo_{(1-x)}O$; the red, green and blue bars in Figure 3), each of the three reaction mechanisms displays a unique trend (Figure 3). For Li:Co_3O_4, the reaction energy increases with increasing Li, which suggests that, at least thermodynamically, higher Li concentrations in $Li_xCo_{(1-x)}O$ should be attainable. In contrast, the opposite trend is observed for 2Li:Co_3O_4; while in the case of 3Li:Co_3O_4, the reaction energy is unaffected by the Li dopant concentration considered. These results suggest that the reaction mechanism for Li metal and Co_3O_4 is likely to change based on the concentration of Li in $Li_xCo_{(1-x)}O$. A complete understanding of these mechanisms requires a range of factors, including reaction conditions and the interfaces of and between Li metal and Co_3O_4, to be accounted. Such simulations are currently being developed in our research groups and are expected to reveal crucial insights into the mechanochemistry of alkali metal and metal oxides. For comparison, we also considered the energetics of the conventional solid-state reaction between Li_2O_2 and CoO used to synthesize $Li_xCo_{(1-x)}O$.[37–39] As shown in Figure S6, the energies for this reaction, from −0.94 to −1.18 eV, are consistently less favorable than the reaction energies presented in Figure 3 for Li metal and Co_3O_4. This

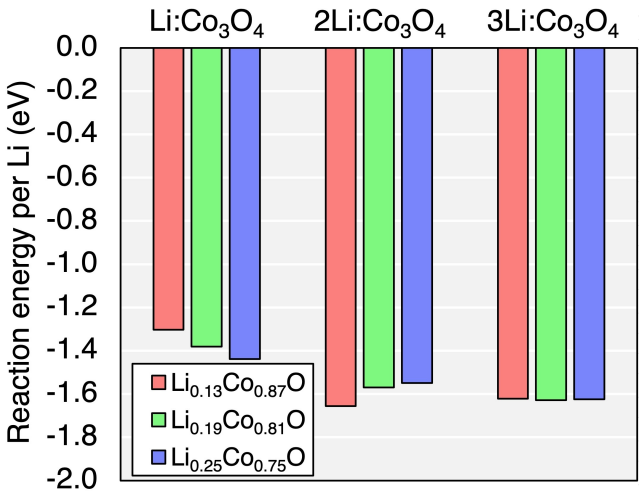

Figure 3. Calculated energies for reactions between Li metal and Li:Co_3O_4 as a function of the Li:Co_3O_4 ratio and Li doping concentration.

Research Article
doi.org/10.1002/ejic.202300344

further evidences the potential of using Li metal as a starting material for the synthesis of lithium transition metal oxides materials. Moreover, Bader charge analysis[40] of the lowest energy $Li_xCo_{(1-x)}O$ configurations from the DFT calculations were conducted, to understand the changes of formal charges for Li, Co and O as a function of Li^+ doping concentration (x) (Figures S8). The biggest charge change was observed for O (11.33 %), followed by Co (5.05 %), while the Bader charge of Li (~0.89 e) remains relatively constant at all doping concentrations. These findings suggest a significant level of oxygen oxidation (from −1.27 e at x = 0 to −1.14 e at x = 0.44), in addition to the expected Co oxidation (from 1.27 e at x = 0 to 1.33 e at x = 0.44), as a result of Li^+ doping. Similar results have been observed previously using X-ray photoelectron spectroscopy for both the Li doping of CoO[41] and the deintercalation of Li^+ from $LiCoO_2$.[42]

Our combined experimental and computational studies suggest that the formation of $Li_xCo_{(1-x)}O$, i.e., Li^+ doping, is preferable with a lower Li metal stoichiometric ratio. On this basis, it is sensible to extrapolate that, instead of a one-pot Li: Co_3O_4 3:1 reaction, introducing the three equivalents of Li metal in a sequential manner would improve the production of $Li_xCo_{(1-x)}O$. Indeed, we found that the sequential reaction not only increased the $Li_xCo_{(1-x)}O$ wt.%, but also produced doped materials with higher Li contents (higher x value), such as $Li_{1.47}Co_3O_{3.72}$, $Li_{0.62}CoO_2$ and $LiCoO_2$ (Figure 4). In comparison, for the one-pot reactions, even with three equivalents of Li metal, the highest Li-content is $Li_{0.185}Co_{0.815}O$. The presence of unreacted Li-metal in the 3:1 one-pot reaction proved that the $Li_{0.185}Co_{0.815}O$ is the highest possible Li-content in the one-pot context. The limit, nonetheless, was overcome by the sequential reactions. We also noticed that, different from the one-pot reactions, the CoO was not observed during the sequential reactions.

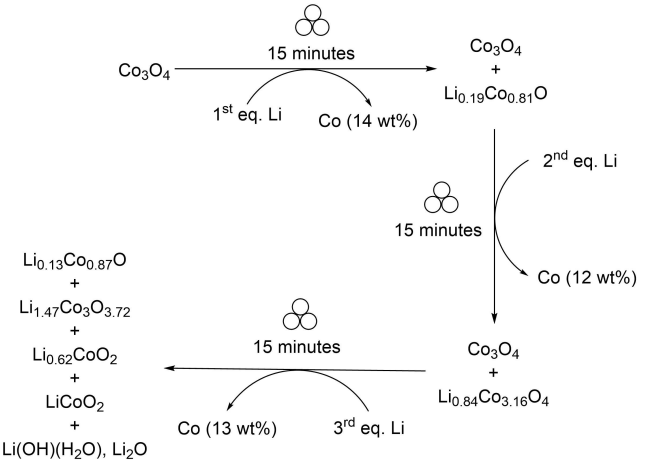

Figure 4. Stepwise reactions between Li metal and Co_3O_4.

Conclusions

By introducing mechanochemical ball milling as an efficient energy input and Li metal as a reductant and Li^+ source, we have provided proof of concept for facile (room temperature, 15–20 min) and controllable reduction and doping of transition-metal oxides. Compared to the state-of-the-art energy-intense methods, this new mechanochemical approach features substantial potential in reducing the carbon footprint. Future work is underway to expand the MO_x scope, as well as employing this novel approach in preparing Li-ion battery cathode materials.

Experimental Section

Materials and instruments: The mechanochemical reactions were conducted using a Retsch™ MM400 mixer mill with a 25 mL Teflon™ reaction jar (screw-and-thread sealing) and a 10 mm-diameter Teflon™ coated steel ball. The reactants (Li metal, NiO or Co_3O_4) are loaded into the reaction jar in a Vigor™ glovebox (argon atmosphere; O_2 and H_2O < 1.0 ppm), together with the milling ball. The lithium metal was used either as plates (approximately 5×5×0.5 mm) or small grains (approximately 1×2×1 mm). The NiO and Co_3O_4 (powder, < 10 μm) were purchased from Merck, dried at 80 °C under dynamic vacuum and stored in the glovebox.

General mechanochemical protocol: ***Caution!*** *The ball milling reactions are exothermic, therefore a cautious approach should be taken by stopping the ball milling intermittently and checking the temperature of the jar. The reactions should never be left unattended, otherwise thermal runaway is likely to take place.*

The 25 mL Teflon™ reaction jar and the ball were pre-dried in 75 °C oven overnight before use. In the glovebox, 10 mmol of NiO/Co_3O_4 and the corresponding amount of Li metal were loaded into the jar, sealed, brought out of the glovebox, and loaded on the MM400 mixer mill. The ball milling reactions were conducted at 20 Hz frequency for an overall reaction time of 15 minutes. A cautious and intermittent approach was adopted for the exothermic reaction: the reactions were stopped every 0.5–1 minutes and the jar's temperature was checked. After the reactions, the jar was taken into the glovebox, where the products were stored. The Co metal grains/ingots and the powdery products were separated by a sieve and a magnet.

Powder X-ray Diffraction (PXRD) data were collected using a Panalytical XPert Pro MPD with an Xcelerator detector using Cu Kα radiation, with a $K\alpha_{1:2}$ ratio of 1:0.5 respectively. A secondary monochromator was used to limit the fluorescence from the presence of cobalt within the samples. Air-sensitive samples were mounted in a glove box, and sealed to the Si zero background holder with Scotch Magic™ Tape. All data were evaluated using the Malvern Panalytical HighScore Plus software package (V5.1), comparing to reference patterns from the Crystallography Open Database (COD).[43] The data were analysed further with Rietveld methods to determine standardless, quantitative phase analysis using HighScore Plus.

A Jeol JSM 5610LV fitted with an Oxford Instruments INCA x-act EDX detector, was used for the EDX analysis of the sample. The sample was mounted on an aluminium stub fitted with a double-sided carbon sticker. The EDX analysis of the Co metal grain/ingot was carried out on five different areas of the sample at a magnification of x500 and using a beam voltage of 20 kV, a working distance of 20 mm and spot size 49.

Research Article
doi.org/10.1002/ejic.202300344

Ball milling reactions between Li metal and NiO: The 1:1 (Li : NiO), 2:1 and 3:1 reactions are conducted following the same protocol, hence are summarized here. In the glovebox, NiO (351 mg, 4.7 mmol) and corresponding amount of Li metal pieces were mixed in the reaction jar. The reaction was ball milled (20 Hz) for 15 minutes. . After 5 minutes, the jar started slightly warming up and continued for 4–5 minutes. The warming-up procedure is irrelevant to the Li:NiO stoichiometric ratio. After the reactions, the powdery mixtures were subjected to PXRD studies. The results are summarized in Figure 1.

Ball milling reactions between Li metal and Co_3O_4

Li:Co_3O_4 = 1:1

In the glovebox, Co_3O_4 (2.568 g, 10.66 mmol) and Li metal (0.074 g, 10.66 mmol) were mixed in the reaction jar. The reaction was ball milled (20 Hz) for 15 minutes. After 5 minutes, the jar started warming up and continued for 4–5 minutes. The mixture of products (2.250 g) was separated into the Co metal grains (0.524 g) and the black powder (1.726 g) by collecting the Co metal grains with a magnet. The outer shell of Co metal grains are briefly polished by sonicating with presence of sands and passing through a plastic sieve.

Li:Co_3O_4 = 2:1

Follow the procedure of the 1:1 reaction, Co_3O_4 (2.323 g, 9.65 mmol) and Li metal (0.184 g, 19.36 mmol) produced Co metal ingots (0.742 g) and the black powder (1.305 g). The reaction jar was warmed up after 5 minutes of ball milling, and cooled to room temperature in 10–15 minutes.

Li:Co_3O_4 = 3:1

Follow the procedure of the 1:1 reaction, Co_3O_4 (2.133 g, 8.86 mmol) and Li metal (0.143 g, 26.58 mmol) produced Co metal ingots (0.430 g) and the black powder (1.911 g). The reaction jar was warmed up after 3 minutes of ball milling: the temperature was significantly higher than the 1:1 or 2:1 reactions. In 15 minutes. The jar was cooled to room temperature.

Sequential Reactions: Follow the procedure of the one pot reactions, Co_3O_4 (1.89 g, 7.87 mmol) was treated with 0.54 g of Li metal (7.87 mmol) under 20 Hz for 15 minutes. The products were sieved and the resultant black powder was treated with another one equivalent of Li metal (0.54 g, 7.87 mmol). The process was repeated for one more time, where in total 3 equivalent of Li metal was introduced.

EDX SEM Characterization of the cobalt metal phase produced by ball milling reactions between Li metal and Co_3O_4: Cobalt metal ingots with a variety of sizes (1–5 mm) were produced by the 1:1 (Li : Co_3O_4) and 2:1 reactions. The metal ingots were isolated from the mixture using a magnet, which were initially covered with a shell of black materials (a mixture of unreacted Co_3O_4, Li_xCo_yO and Li_2O). The black covering materials were removed by sandpaper to expose the silvery metallic surfaces, which were subjected to SEM EDX analysis with multiple spots to understand the elemental components of the metallic phase. The metal ingots from 1:1 and 2:1 reactions were found to have similar elemental components of their metallic phases, which are comprised of $>80\%$ Co, with the rest are C (~7%) and O (~9%). See Tables S1–S5 and Figures S1–S6 for the representative results.

Powder X-Ray Diffraction (PXRD): Phase identification of experimental materials was performed by PXRD utilising a PANalytical X'Pert Pro MPD, powered by a Philips PW3040/60 X-ray generator fitted with an X'Celerator detector. Diffraction data were acquired by exposing powder samples to Cu–Kα X-ray radiation, which has a characteristic wavelength (λ) of 1.5418 Å. X-rays were generated from a Cu anode supplied with 40 kV and a current of 40 mA. Datasets were collected step size of 0.0334° 2θ and nominal time per step of 1 s, using the scanning X'Celerator detector and a Ni Kβ filter in the diffracted beam path. When the samples contained Co which fluoresce in copper radiation, a secondary monochromator was used to reduce the observed fluorescence.

PXRD Sample preparation: As all of the samples were sensitive to reaction with oxygen/moisture, PXRD sample preparation was perfomed in a N2 glove box. Powdered samples were transferred to a Si zero background holder and were sealed using Scotch Magic™ Tape. Samples were rapidly transferred to the diffractometer for measurement.

PXRD data analysis: The standardless, quantitative phase analysis was completed using Rietveld methods within the Malvern Panalytical HighScore Plus software package. The Rietveld method involves constructing a model consisting of the crystal structures of all component phases, and the differences between the observed and simulated diffraction patterns are minimised by varying scale factors, unit-cell parameters, and crystallite size for each phase. This method provides information on well-ordered (crystalline) phases, and determined the quantitative distribution of the crystalline phases within the powdered samples.

Acknowledgements

The authors thank the Newcastle University Chemistry Technical Support Team (Dr Laura McCorkindale, Dr Amy Roberts and Ms. Alexandra Rotariu) and Mr. Gary Day (Chemistry Mechanical Workshop) for supporting our research. E. L. thanks Profs. Steve Bull and Paul Christensen (School of Engineering, Newcastle University) for insightful discussions. E. L. and J. A. D. thank the Newcastle University Academic Track (NUAcT) Fellowship Scheme for financial support. N. D. thanks Newcastle University for a NUAcT PhD studentship and the Royal Society of Chemistry Research Enablement Grants (E22-3348740748). J. A. D. gratefully acknowledges the EPSRC (EP/V013130/1) for funding. Via membership of the UK's HEC Materials Chemistry Consortium, which is funded by the EPSRC (EP/L000202, EP/L000202/1, EP/R029431 and EP/T022213), this work used the ARCHER UK National Supercomputing Service. E. L. thanks the EPSRC North East Centre of Energy Materials (NECEM) and the Royal Society of Chemistry Research Enablement Grants (E20-5153) for financial support to build the mechanochemistry facility.

Conflict of Interests

The authors declare no conflict of interest.

Data Availability Statement

The data that support the findings of this study are available in the supplementary material of this article.

Keywords: cobalt oxide · doping · lithium · mechanochemistry · nickel oxide · reduction

[1] J. C. Védrine, *ChemSusChem* **2018**, *12*, 577–588.
[2] M. B. Gawande, R. K. Pandey, R. V. Jayaram, *Catal. Sci. Technol.* **2012**, *2*, 1113–1125.
[3] D. Koziej, A. Lauria, M. Niederberger, *Adv. Mater.* **2013**, *26*, 235–257.
[4] A. Rukini, M. A. Rhamdhani, G. A. Brooks, A. van den Bulck, *J. Sustain. Metall.* **2022**, *8*, 1–24.
[5] A. R. Puigdollers, P. Schlexer, S. Tosoni, G. Pacchioni, *ACS Catal.* **2017**, *7*, 6493–6513.
[6] S. B. Ogale, *Adv. Mater.* **2010**, *22*, 3125–3155.
[7] X. Xie, Y. Li, Z.-Q. Liu, M. Heruta, W. Shen, *Nature* **2009**, *458*, 746–749.
[8] Y. Shao-Horn, L. Croguennec, C. Delmas, E. C. Nelson, M. A. O'Keefe, *Nat. Mater.* **2003**, *2*, 464–467.
[9] Y. Shi, X. Pan, B. Li, M. Zhao, H. Pang, *Chem. Eng. J.* **2018**, *343*, 427–446.
[10] L. J. Garces, B. Hincapie, R. Zerger, S. L. Suib, *J. Phys. Chem. C* **2015**, *119*, 5484–5490.
[11] B. Khoshandam, R. V. Kumar, E. Jamshidi, *Metall. Mater. Trans. B.* **2004**, *35b*, 825–828.
[12] S. Cetinkaya, S. Eroglu, *JOM* **2018**, *70*, 2237–2242.
[13] K. C. Sabat, R. K. Paramguru, S. Pradhan, B. K. Mishra, *Plasma Chem. Plasma Process.* **2015**, *35*, 387–399.
[14] L. Luo, J. Wu, J. Xu, V. P. Dracid, *ACS Nano* **2014**, *8*, 11560–11566.
[15] K. V. Manukyan, A. G. Avetisyan, C. E. Shuck, H. A. Chatilyan, S. Rouvimov, S. L. Kharatyan, A. S. Mukasyan, *J. Phys. Chem. C* **2015**, *119*, 16131–16138.
[16] G. Parravano, *J. Am. Chem. Soc.* **1952**, *74*, 1194–1198.
[17] G. X. Wang, S. Bewlay, J. Yao, Y. Chen, Z. P. Guo, H. K. Liu, S. X. Dou, *J. Power Sources* **2003**, *119–121*, 189–194.
[18] J.-L. Do, T. Friščić, *ACS Cent. Sci.* **2017**, *3*, 13–19.
[19] L. Takacs, *Chem. Soc. Rev.* **2013**, *42*, 7649–7659.
[20] E. Boldyreva, *Chem. Soc. Rev.* **2013**, *42*, 7719–7738.
[21] T. Friščić, C. Mottillo, H. Titi, *Angew. Chem. Int. Ed.* **2020**, *59*, 1018–1029.
[22] N. R. Rightmire, T. P. Hanusa, *Dalton Trans.* **2016**, *45*, 2352–2362.
[23] Y. Chen, G. Mellow, D. van Luijk, C. Creton, R. P. Sijbesma, *Chem. Soc. Rev.* **2021**, *50*, 4100–4140.
[24] D. N. Rainer, R. E. Morris, *Dalton Trans.* **2021**, *50*, 8995–9009.
[25] T. Tsuzuki, *Commun. Chem.* **2021**, *4*, 143.
[26] R. Schlem, C. F. Burmeister, P. Michalowski, S. Ohno, G. F. Dewald, A. Kwade, W. G. Zeier, *Adv. Energy Mater.* **2021**, *11*, 2101022.
[27] N. Davison, P. G. Waddell, C. Dixon, C. Wills, T. J. Penfold, E. Lu, *Dalton Trans.* **2022**, *51*, 10707–10713.
[28] N. Davison, K. Zhou, P. G. Waddell, C. Wills, C. Dixon, S.-X. Hu, E. Lu, *Inorg. Chem.* **2022**, *61*, 3674–3682.
[29] N. Davison, E. Falbo, P. G. Waddell, T. J. Penfold, E. Lu, *Chem. Commun.* **2021**, *57*, 6205–6208.
[30] For reviews about using zero-valent metals in mechanochemistry, see: a) A. C. Jones, J. A. Leitch, S. E. Raby-Buck, D. L. Browne, *Nature Synth.* **2022**, *1*, 763–775; b) D. Tan, F. García, *Chem. Soc. Rev.* **2019**, *48*, 2274–2292.
[31] Recent examples using s-block metals in mechanochemistry: a) Y. Gao, K. Kubota, H. Ito, *Angew. Chem. Int. Ed.* **2023**, *62*, e202217723; b) N. Davison, J. A. Quirk, F. Tuna, D. Collison, C. L. McMullin, H. Michaels, G. H. Morritt, P. G. Waddell, J. A. Gould, M. Freitag, J. A. Dawson, E. Lu, *Chem* **2023**, *9*, 576–591; c) P. Gao, J. Jiang, S. Maeda, K. Kubota, H. Ito, *Angew. Chem. Int. Ed.* **2022**, *61*, e202207118; d) D. Jędrzkiewicz, J. Mai, J. Langer, Z. Mathe, N. Patel, S. DeBeer, S. Harder, *Angew. Chem. Int. Ed.* **2022**, *61*, e202200511; e) D. Jędrzkiewicz, J. Langer, S. Harder, *Z. Anorg. Allg. Chem.* **2022**, *648*, e202200138; f) R. Takahashi, A. Hu, P. Gao, Y. Gao, Y. Pang, T. Seo, J. Jiang, S. Maeda, H. Takaya, K. Kubota, H. Ito, *Nat. Commun.* **2021**, *12*, 6691; g) C.-S. Wang, Q. Sun, F. García, C. Wang, N. Yoshikai, *Angew. Chem. Int. Ed.* **2021**, *60*, 9627–9634.
[32] Recent examples using d-block metals in mechanochemistry: a) M. T. J. Williams, L. C. Morrill, D. L. Browne, *Adv. Synth. Catal.* **2023**, *365*, 1477–1484; b) M. Wohlgemuth, M. Mayer, M. Rappen, F. Schmidt, R. Saure, S. Grätz, L. Borchardt, *Angew. Chem. Int. Ed.* **2022**, *61*, e202212694; c) W. Pickhardt, C. Beaković, M. Mayer, M. Wohlgemuth, F. J. L. Kraus, M. Etter, S. Grätz, L. Borchardt, *Angew. Chem. Int. Ed.* **2022**, *61*, e202205003; d) S. Hwang, S. Grätz, L. Borchardt, *Chem. Commun.* **2022**, *58*, 1661–1671.
[33] Recent examples using p-block metals in mechanochemistry: a) A. C. Jones, M. T. J. Williams, L. C. Morrill, D. L. Browne, *ACS Catal.* **2022**, *12*, 13681–13689; b) A. C. Jones, W. I. Nicholson, J. A. Leitch, D. L. Browne, *Org. Lett.* **2021**, *23*, 6337–6341; c) A. C. Jones, W. I. Nicholson, H. R. Smallman, D. L. Browne, *Org. Lett.* **2020**, *22*, 7433–7438; d) O. Dolotko, I. Z. Hlova, Y. Mudryk, S. Gupta, V. P. Balema, *J. Alloys Compd.* **2020**, *824*, 153876; e) Q. Cao, R. T. Stark, I. A. Fallis, D. L. Browne, *ChemSusChem* **2019**, *12*, 2554–2557; f) Q. Cao, J. L. Howard, E. Wheatley, D. L. Browne, *Angew. Chem. Int. Ed.* **2018**, *57*, 11339–11343.
[34] L. L. Wang, Z. A. Munir, Y. M. Maximov, *J. Mater. Sci.* **1993**, *28*, 3693–3708.
[35] W. Liu, P. Oh, X. Liu, M. J. Lee, W. Cho, S. Chae, Y. Kim, J. Cho, *Angew. Chem. Int. Ed.* **2015**, *54*, 4440–4457.
[36] P. M. Zehermaier, A. Cornélis, F. Zoller, B. Böller, A. Wisnet, M. Döblinger, D. Böhm, T. Bein, D. Fattakhova-Rohlfing, *Chem. Mater.* **2019**, *31*, 8685–8694.
[37] W. D. Johnston, R. R. Heikes, D. Sestrich, *J. Phys. Chem. Solids* **1958**, *7*, 1–13.
[38] Y. Wu, D. Pasero, E. E. McCabe, Y. Matsushima, A. R. West, *J. Mater. Chem.* **2009**, *19*, 1443–1448.
[39] E. Antolini, *J. Phys. D* **1998**, *31*, 334–335.
[40] G. Henkelman, A. Arnaldsson, H. A. Jonsson, *Comput. Mater. Sci.* **2006**, *36*, 354–360.
[41] J. van Elp, J. L. Wieland, H. Eskes, P. Kuiper, G. A. Sawatzky, *Phys. Rev. B* **1991**, *44*, 6090–6103.
[42] L. Dahéron, R. Dedryvère, H. Martinez, M. Ménétrier, C. Denage, C. Delmas, D. Gonbeau, *Chem. Mater.* **2008**, *20*, 583–590.
[43] S. Grazulis, D. Chateigner, R. T. Downs, A. T. Yokochi, M. Quiros, L. Lutterotti, E. Manakova, J. Butkus, P. Moeck, A. Le Bail, *J. Appl. Crystallogr.* **2009**, *42*, 726–729.

Manuscript received: June 3, 2023
Revised manuscript received: September 7, 2023
Accepted manuscript online: October 6, 2023
Version of record online: ■■, ■■

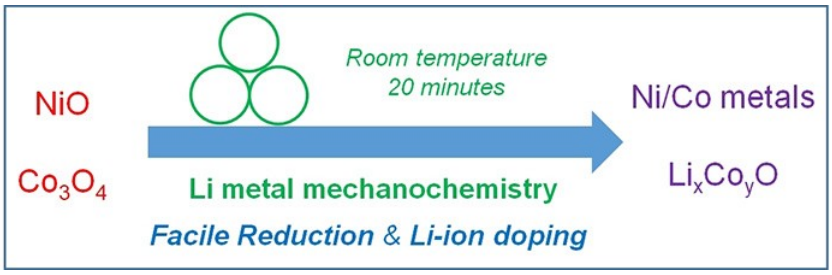

N. Davison, T. Khatun, Dr. I. Arce-Garcia, Dr. J. A. Gould, Dr. J. A. Dawson*, Dr. E. Lu**

1 – 7

Facile Mechanochemical Reduction and Lithium-Ion Doping of Transition-Metal Oxides[]

Reduction and Li-ion doping of metal oxides are important but notoriously difficult. Herein, by introducing Li-metal into mechanochemistry, we report facile reduction and Li-ion doping (for Co_3O_4) of cobalt and nickel oxides, namely, Co_3O_4 and NiO.